SYMMETRIC BEM FOR FRACTURE MECHANICS OF THIN PLATES

A. FRANGI* and G. NOVATI**
*Dept. of Structural Engineering, Politecnico di Milano, P.zza Leonardo da Vinci 32, 20133 Milan, Italy
**Dept. of Structural Mechanics and Design Automation, University of Trento, via Mesiano 77, 38050 Trento, Italy

ABSTRACT

A direct Symmetric Galerkin Boundary Element Method for the analysis of fractures in thin (Kirchhoff) infinite elastic plates in bending is presented as a particular case of a general formulation. Numerical difficulties due to the presence of highly singular integrals are overcome exploiting an analytical regularization procedure. Only weakly singular double integrals need to be computed. Two topics are addressed: evaluation of the stress intensity factors from the near-tip displacement and normal-slope fields and computation of the energy release rate by means of a sensitivity analysis procedure. In order to obtain a better accuracy special tip elements have been developed allowing to simulate the correct asymptotic behaviour of the variables involved. The procedure outlined can be applied to arbitrary crack shapes: numerical examples are provided for straight and circular fractures in infinite plates subject to bending moments and vertical shears. Comparisons between analytical and numerical results validate the ideas presented in this contribution.

KEYWORDS

Kirchhoff plates, symmetric BEM, stress intensity factors, energy release rate

INTRODUCTION

One of the most appealing features of the Symmetric Boundary Element formulations in 2D and 3D elasticity and potential problems (Sirtori, 1979; Maier and Polizzotto, 1987; Nishimura and Kobayashi, 1991; Sirtori *et al.*, 1992; Maier *et al.*, 1993; Bonnet, 1996) is their capability to simulate fractures without requiring special interfaces (unlike usual Collocation formulations), or particular 'discontinuous' elements which are necessary in the so called Dual Approach (Portela, 1993). The use of the traction equation, in fact, ideally lends itself to the enforcement of boundary conditions along cracks. Moreover, the presence of strongly singular and hypersingular integrals is no serious drawback since regularization procedures have been devised (Nishimura and Kobayashi, 1991; Sirtori *et al.*, 1992; Bonnet, 1995; Frangi and Novati, 1996) which reduce the order of singularity so that only weakly singular integrals need to be evaluated numerically. Recently, in the context of the Kirchhoff-plates theory, two new BE methods have been proposed: a regularized collocation approach (Frangi, 1996) and a symmetric variational formulation based on an augmented potential energy functional (Frangi and Bonnet, 1996). A symmetric BE formulation for fracture mechanics can be more directly obtained starting from a Betti statement, in which the auxiliary state is generated by a suitable distribution of static sources (forces and moments) and kinematic sources (vertical displacement and normal-slope discontinuities). The latter approach is followed in this paper allowing the mathematical idealization of fractures as lines which are loci of vertical displacement and normal-slope discontinuities.

SYMMETRIC GALERKIN BE FORMULATION

The behaviour of a thin plate of boundary Γ_E with a crack Γ inside, which is small in comparison to the plate dimensions, can be usefully represented considering the crack Γ in an unbounded domain.

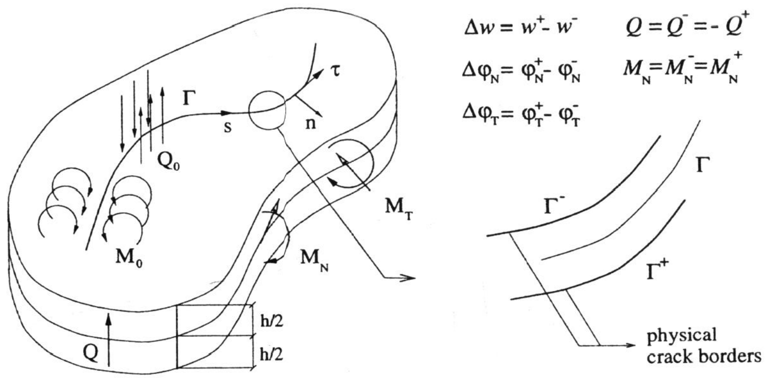

Fig. 1 Relevant notation and conventions

Only Γ is discretized under the hypothesis that the real elastic state satisfies suitable (radiation) conditions at infinity. The governing variational equation can be obtained as the particular case of a general formulation which is developed in a parallel paper (Frangi, 1997) and reads (considering a smooth crack with no corners and zero normal pressure):

$$\int_\Gamma [Q_K \Delta\tilde{w} - M_N \Delta\tilde{\varphi}_N + \delta M_N \Delta\varphi_N + \delta M_T \Delta\varphi_T - \delta Q \Delta w]\, \mathrm{d}s = 0 \qquad (1)$$

In eq.(1) Δw denotes the vertical displacement discontinuity $w^+ - w^-$ along Γ (see Fig. 1), $\Delta\varphi_N = \Delta w_{,i} n_i$ and $\Delta\varphi_T = \Delta w_{,i}\tau_i$ the normal- and tangential-slope discontinuities, $M_N = M_{ij} n_i n_j$ the normal moment acting on both sides of Γ, $M_T = M_{ij} n_i \tau_j$ the twisting moment and Q_K the Kirchhoff equivalent shear defined as $Q_K = Q + \frac{\partial M_T}{\partial s}$ where $Q = Q_i n_i$ is the pure shear and s is the arc length along Γ (the comma indicates partial differentiation with respect to the field point and the Einstein summation convention is adopted for lower-case indices). The moment and shear components are defined from the three-dimensional

stress tensor as:

$$M_{ij}(\boldsymbol{x}) \equiv \int_{-h/2}^{h/2} \sigma_{ij}(\boldsymbol{x}, z) z\, \mathrm{d}z = -K_{ijk\ell} w_{,k\ell} \qquad Q_i(\boldsymbol{x}) \equiv \int_{-h/2}^{h/2} \sigma_{i3}(\boldsymbol{x}, z)\, \mathrm{d}z = M_{ij,j} = -D w_{,ijj}$$

$$K_{ijk\ell} = D[(1-\nu)\delta_{ik}\delta_{j\ell} + \nu\delta_{ij}\delta_{k\ell}] \quad \{i,j\} \in (1,2) \qquad D = \frac{Eh^3}{12(1-\nu^2)}$$

The auxiliary state, denoted by $\delta(\cdot)$, is generated by a distribution of normal-slope discontinuities $\Delta\tilde{\varphi}_N$ and displacement discontinuities $\Delta\tilde{w}$ on Γ.
Since δQ can be expressed as $\delta Q = \frac{\partial \delta R}{\partial s}$ (Frangi and Bonnet, 1996), letting $\delta P_{ij} = \delta M_{ij} - e_{ij}\delta R$, eq.(1) may be rewritten as:

$$\int_\Gamma [Q_K \Delta\tilde{w} - M_N \Delta\tilde{\varphi}_N + \delta P_{ij} n_j \Delta w_{,i}]\, \mathrm{d}s = 0 \qquad (2)$$

where the identity: $\delta M_{ij} n_j \Delta w_{,i} = \delta M_N \Delta\varphi_N + \delta M_T \Delta\varphi_T$ has been used. In (Frangi and Bonnet, 1996) it is shown that:

$$\delta P_{ij}(\boldsymbol{x}) n_j = \int_\Gamma \frac{\partial}{\partial s}\frac{\partial}{\partial \tilde{s}} Z_{ik}(\boldsymbol{x}, \tilde{\boldsymbol{x}}) \Delta\tilde{w}_{,k}(\tilde{\boldsymbol{x}})\, \mathrm{d}s_{\tilde{x}} \qquad (3)$$

with:

$$Z_{ik}(\boldsymbol{x}, \tilde{\boldsymbol{x}}) = -D^2\left[(1-\nu^2) W_{,a\tilde{a}}(\boldsymbol{x}, \tilde{\boldsymbol{x}})\delta_{ik} + (1-\nu)^2 W_{,i\tilde{k}}(\boldsymbol{x}, \tilde{\boldsymbol{x}})\right] \qquad (4)$$

where $\frac{\partial}{\partial \tilde{s}}$ denotes differentiation with respect to the arc length defining the $\tilde{\boldsymbol{x}}$ position and the comma followed by a tilded lower case letter denotes differentiation with respect to the corresponding $\tilde{\boldsymbol{x}}$ coordinate. Moreover $W(\boldsymbol{x}, \tilde{\boldsymbol{x}})$ is the displacement induced at $\boldsymbol{x}$ by a unit vertical force acting at $\tilde{\boldsymbol{x}}$ and is given by:

$$W(\boldsymbol{x}, \tilde{\boldsymbol{x}}) = \frac{1}{16\pi D}(r^2 \mathrm{Log} r^2 - r^2) \qquad r = |\tilde{\boldsymbol{x}} - \boldsymbol{x}| \qquad (5)$$

Through integrations by parts, if $\Delta w_{,i}$ and $\Delta\tilde{w}_{,i}$ are C^0 on Γ:

$$\int_\Gamma \Delta w_{,i}(\boldsymbol{x}) \delta P_{ij}(\boldsymbol{x}) n_j(\boldsymbol{x})\, \mathrm{d}s_x = \int_\Gamma \int_\Gamma \frac{\partial}{\partial s}\Delta w_{,i}(\boldsymbol{x}) Z_{ik}(\boldsymbol{x}, \tilde{\boldsymbol{x}}) \frac{\partial}{\partial \tilde{s}}\Delta\tilde{w}_{,\tilde{k}}(\tilde{\boldsymbol{x}})\, \mathrm{d}s_{\tilde{x}}\, \mathrm{d}s_x = \mathcal{B}(\Delta w, \Delta\tilde{w})$$

It is worth mentioning that, once the regularization has been performed, the cartesian gradients might be replaced, if necessary, by the 'physical' fields $\Delta\varphi_T$ and $\Delta\varphi_N$ since, for instance: $\frac{\partial}{\partial s}\Delta w = D_i^T \Delta\varphi_T + D_i^N \Delta\varphi_N$ having defined the operators:

$$D_a^N f(\boldsymbol{x}) \stackrel{Def}{=} \left[n_a \frac{\partial}{\partial s} f - \frac{1}{\rho}\tau_a f\right](\boldsymbol{x}) \qquad D_a^T f(\boldsymbol{x}) \stackrel{Def}{=} \left[\tau_a \frac{\partial}{\partial s} f + \frac{1}{\rho} n_a f\right](\boldsymbol{x})$$

where ρ is the curvature radius of Γ.
Note that, according to the Kirchhoff approximation, $\Delta\varphi_T$ is the tangential derivative of Δw. It is thus possible to deal indifferently either with Δw, interpolated via C^1 cubic hermitian shape functions, or with $\Delta\varphi_T$, interpolated via C^0 quadratic lagrangian shape functions. If the latter choice is made 'compatibility' must be checked, i.e. $\int \Delta\varphi_T\, \mathrm{d}s$ should represent an admissible displacement field (e.g. if a crack is considered, the resulting displacement discontinuity must vanish at the crack tips).

ENERGY RELEASE RATE EVALUATION

The total potential energy functional for a crack in an infinite plate under uniform bending moments M_0 and shear Q_0 (see Fig. 1) is:

$$T = \frac{1}{2}\mathcal{B}(\Delta w, \Delta w) - M_0 \int_\Gamma \Delta w_{,i}(\boldsymbol{x}) n_i \, ds_x + Q_0 \int_\Gamma \Delta w(\boldsymbol{x}) \, ds_x \tag{6}$$

The energy release rate due to a crak-tip extension is computed as the material derivative of eq.(6) with respect to the coordinates of the crack-tip involved. A "transformation velocity" $\boldsymbol{\vartheta}$ is introduced, defining the deformation process (extension) of the crack tip. Let $\overset{\star}{(\cdot)}$ represent the material (lagrangian) derivative operator with respect to a generic shape parameter p (Dems and Mróz, 1983; Bonnet, 1996). Applying this operator to the differential line element ds (with $\boldsymbol{\tau}$ tangent versor): $\overset{\star}{ds} = (\boldsymbol{\tau}\cdot\nabla\boldsymbol{\vartheta}\cdot\boldsymbol{\tau})\, ds = \frac{\partial}{\partial s}(\vartheta_i \tau_i)\, ds$. Since $\Delta \overset{\star}{w}$ represents an admissible displacement field, from the variational equation eq.(2):

$$\mathcal{B}(\Delta \overset{\star}{w}, \Delta w) - M_0 \int_\Gamma \Delta \overset{\star}{w}_{,i}(\boldsymbol{x}) n_i \, ds_x + Q_0 \int_\Gamma \Delta \overset{\star}{w}(\boldsymbol{x}) \, ds_x = 0 \tag{7}$$

It can be shown that the material derivatives $\overset{\star}{T}$ is then given by:

$$\overset{\star}{T} = \mathcal{D}(\Delta w_{,j}\theta_j, \Delta w) + \frac{1}{2}\int_\Gamma \int_\Gamma \frac{\partial}{\partial s}\Delta w_{,i}(\boldsymbol{x}) \, \overset{\star}{Z}_{ik}(\boldsymbol{x}, \tilde{\boldsymbol{x}}) \frac{\partial}{\partial \tilde{s}} \Delta \tilde{w}_{,\tilde{k}}(\tilde{\boldsymbol{x}}) \, ds_{\tilde{x}} \, ds_x$$
$$- M_0 \int_\Gamma \Delta w_{,i}(\boldsymbol{x}) \, (n_i \overset{\star}{ds_x}) + Q_0 \int_\Gamma \Delta w(\boldsymbol{x}) \, \overset{\star}{ds_x} \tag{8}$$

with:

$$\mathcal{D}(\Delta w_{,j}\theta_j, \Delta w) = -\mathcal{B}(\Delta w_{,j}\vartheta_j, \Delta w) + M_0 \int_\Gamma \Delta w_{,j}(\boldsymbol{x}) \vartheta_{j,i}(\boldsymbol{x}) n_i \, ds_x \tag{9}$$

Note that, if $Q_0 = 0$, $\mathcal{D}(\Delta w_{,j}\theta_j, \Delta w) = 0$, according to eq.(2). In this specific case $\boldsymbol{\vartheta}$ is chosen such that $\boldsymbol{\vartheta} = \vartheta\boldsymbol{\tau}$; moreover it has non-zero values only on the tip-element where it displays a linear variation from 1 (crack tip) to 0. Under these hypotheses $\overset{\star}{T}$ represents the energy release rate G. Denoting by k_1 and k_2 the stress intensity factors, G can be computed from the near-tip fields as (Hui and Zehnder, 1993):

$$G = (k_1^2 + k_2^2) \frac{h^4 \pi}{36 D (3 + \nu)(1 - \nu)} \tag{10}$$

SPECIAL TIP ELEMENTS

The near-tip displacement field w, in polar coordinates, reads (Hui and Zehender, 1993):

$$w = \frac{(2r)^{\frac{3}{2}} h^2}{24 D (3+\nu)} \left\{ k_1 \left[\frac{1}{3}\frac{7+\nu}{1-\nu} \cos(\frac{3}{2}\vartheta) - \cos(\frac{1}{2}\vartheta) \right] + k_2 \left[\frac{1}{3}\frac{5+3\nu}{1-\nu} \sin(\frac{3}{2}\vartheta) - \sin(\frac{1}{2}\vartheta) \right] \right\} + o(r^{\frac{3}{2}}) \tag{11}$$

An accurate numerical evaluation of the stress intensity factors and of the energy release rate requires the developement of special tip elements, in the same spirit of those used in 2D linear elastic fracture mechanics (Aliabadi, 1991). In fact, the near-tip displacement and normal-slope discontinuity fields cannot be suitably represented if usual discretization hypotheses are adopted, i.e. lagrangian quadratic and cubic hermitian shape functions

modelling the normal-slope and the vertical displacement fields and "linear" elements modelling the geometry. Here "linear" means that the current point position is given, over one element, as a linear combination of the two end points coordinates by means of an intrinsic parameter η ($\eta \in -1, 1$). For instance a circular arc element of span $\Delta\beta$ (on which the point coordinates are completely defined by the radius R and the angle β) is said to be "linear" if the point angle is determined through a linear combination of the two end-point angle values. In 2D LEFM one of the most frequently used procedures consists in introducing a modified element geometry description (quarter point element): let $\eta = 1$ and $\eta = -1$ correspond to the crack tip $\mathbf{P}_1$ and to the second element end-point $\mathbf{P}_{-1}$ respectively; denote by $\mathbf{P}_{1/2}$ the point corresponding to $\eta = \frac{1}{2}$ in the linear element defined by $\mathbf{P}_{-1}$ and $\mathbf{P}_1$. In the modified element the point coordinates (angle value for arc elements) are described in terms of a quadratic lagrangian interpolation of the coordinates of three points: the two end nodes and $\mathbf{P}_{1/2}$.
This technique can been succesfully applied to thin plates if the extrapolation is made in terms of the normal-slope field. Let ρ denote the distance along the element of a point from the crack tip ($\rho \equiv r$ for straight elements and $\rho \equiv R(\beta_{P_1} - \beta)$ for circular arc elements):

$$\rho = \frac{L}{4}(1-\eta)^2 \qquad J = \frac{L}{2}(1-\eta) = \sqrt{L\rho} \tag{12}$$

where J is the jacobian of the transformation $\rho = \rho(\eta)$ and L is the distance between the two end points in the case of straight elements and $L = R\Delta\beta$ for arc elements. From eq.(11) the near-tip normal-slope displacement discontinuity is:

$$\Delta\varphi_N(r) = \frac{1}{r}\frac{\partial w}{\partial \vartheta}\Big|_{\vartheta=-\pi}^{\vartheta=\pi} = \frac{2\sqrt{2}k_1 \rho^{1/2} h^2}{3D(3+\nu)(1-\nu)} + o(\rho^{1/2}) \tag{13}$$

The interpolation of $\Delta\varphi_N$ on the modified tip element, using eq.(12), becomes:

$$\Delta\varphi_N = (4\Delta\varphi_{N,1/2} - \Delta\varphi_{N,-1})\sqrt{\frac{\rho}{L}} + 2(\Delta\varphi_{N,-1} - 2\Delta\varphi_{N,1/2})\frac{\rho}{L} \tag{14}$$

where $\Delta\varphi_{N,-1}$ and $\Delta\varphi_{N,1/2}$ are the normal-slope discontinuity values at $\mathbf{P}_{-1}$ and $\mathbf{P}_{1/2}$ respectively. Thus the required $\rho^{1/2}$ variation near the crack tip is obtained.
On the contrary, if the Δw field is modelled and the extrapolation is based on the displacement or tangential-slope fields, the modified tip element does not provide the required behaviour, as explained by the following remarks. From eq.(11) the near-tip displacement and tangential-slope discontinuities read:

$$\Delta w = \frac{4\sqrt{2}k_2 \rho^{3/2} h^2}{9D(3+\nu)(1-\nu)} + o(\rho^{3/2}) \qquad \Delta\varphi_T = \frac{2\sqrt{2}k_2 \rho^{1/2} h^2}{3D(3+\nu)(1-\nu)} + o(\rho^{1/2}) \tag{15}$$

Neither a linear element, nor the "quarter point element" previously described can be applied in modelling the crack tip. In fact these choices would lead to $\Delta w = O(\rho^2)$ and $\Delta w = O(\rho)$ respectively. In this paper the following "composite" technique has been adopted: the geometry is still described by means of the singular "quarter" point element (which is needed in order to guarantee the correct representation for the normal-slope field) and modified quartic polinomial functions are used in modelling the displacement field:

$$\Delta w = C_3(1-\eta)^3 + C_4(1-\eta)^4 = C_3(\frac{2\rho}{L})^{3/2} + C_4(\frac{2\rho}{L})^2 \tag{16}$$

The term $C_4(1-\eta)^4$ is required in order to comply with the continuity requisites imposed on both the displacement and tangential-slope discontinuity fields. Using eq.(16) it is in fact possible to determine two shape functions such that, in $\eta = -1$, $\Delta w = 1$; $\frac{\partial \Delta w}{\partial \eta} = 0$ and $\Delta w = 0$; $\frac{\partial \Delta w}{\partial \eta} = 1$ respectively.

Straight crack subject to constant normal bending moments M_0

Let us consider a straight crack of length $2a$ in an infinite plate subject to constant normal bending moments M_0 (see Fig. 1). Following Hui and Zehnder (1993):

$$k_1 = \frac{6M_0}{h^2}\sqrt{a} \qquad k_2 = 0 \tag{17}$$

Numerical investigations have been carried out with different mesh-refinements using both linear and modified crack-tip elements.

	$k_1^{M_0}\frac{h^2}{M_0 a^{1/2}}$	rel. err.	$k_{2,w}^{Q_0}\frac{h^2}{Q_0 a^{3/2}}$	rel. err.	$k_{2,\varphi T}^{Q_0}\frac{h^2}{Q_0 a^{3/2}}$	rel. err.
Exact	6.		3.		3.	
M_{10}	5.9455	9.06E-03	2.7464	8.45E-02	2.7389	8.70E-02
M_{20}	5.9757	4.05E-03	2.8303	5.65E-02	2.8786	4.04E-02
S_{10}	5.9844	2.25E-03	2.9027	3.24E-02	2.8541	4.86E-02
S_{20}	5.9992	1.29E-04	2.9998	6.50E-05	3.0016	5.46E-04

Table 1: Straight crack: adimensional stress intensity factors

The results are presented for four cases: mesh M_{10} with 10 linear elements; mesh M_{20} with 20 linear elements; meshes S_{10} and S_{20} with the same modelling as for M_{10} and M_{20} but with modified crack-tip elements. In the first two columns of Table 1 the stress intensity factors are compared with the exact solution.

	$G^{M_0}D/(M_0^2 a)$	rel. err.	$G^{Q_0}D/(Q_0^2 a^3)$	rel. err.
Exact	.1360E+01		.3400E+00	
M_{10}	.1303E+01	-.419E-01	.3246E+00	-.451E-01
M_{20}	.1305E+01	-.401E-01	.3266E+00	-.393E-01
S_{10}	.1360E+01	.453E-03	.3377E+00	-.648E-02
S_{20}	.1360E+01	.508E-03	.3403E+00	.113E-02

Table 2: Straight crack: adimensional energy release rates

The numerical values of the stress intensity factors are obtained through evaluation of eq.(13) in the middle node of the the crack-tip element without any data-fitting procedure. In Table 2, on the contrary, are collected the numerical results of the energy release rates computed using the same meshes previously described.

Straight crack subject to constant shear Q_0

The same plate as in the previous example is now subject to constant shear Q_0.

The stress intensity factors are (Hui and Zehnder, 1993):

$$k_1 = 0 \qquad k_2 = \frac{3Q_0}{h^2}a^{3/2} \tag{18}$$

Numerical investigations have been carried out with different mesh-refinements using both linear and special crack-tip elements and the same discretizations as in the normal moment example. The numerical values of the stress intensity factors (Table 1) are obtained through evaluation of eq.(15) in the first node of the the crack-tip element. Two approximations of k_2 are provided using either the displacement discontinuity ($k_{2,w}$ column) or the tangential-slope field ($k_{2,\varphi T}$ column). The results concerning the energy release rate computations are collected in Table 2.

	$k_1h^2/(M_0R^{1/2})$	rel. err.	$k_2h^2/(M_0R^{1/2})$	rel. err.
Exact 20°	.3477E+01		.6132E+00	
M_{10}, 20°	.3299E+01	.512E-01	.5941E+00	.312E-01
M_{20}, 20°	.3353E+01	.357E-01	.5937E+00	.317E-01
S_{10}, 20°	.3461E+01	.471E-02	.6224E+00	-.150E-01
S_{20}, 20°	.3490E+01	-.352E-02	.6178E+00	-.746E-02
Exact 70°	.5121E+01		.3586E+01	
M_{10}, 70°	.4831E+01	.566E-01	.3475E+01	.310E-01
M_{20}, 70°	.4933E+01	.368E-01	.3472E+01	.317E-01
S_{10}, 70°	.5070E+01	.100E-01	.3640E+01	-.152E-01
S_{20}, 70°	.5134E+01	-.246E-02	.3613E+01	-.748E-02

Table 3: Arc crack: adimensional stress intensity factors

Arc crack subject to constant normal bending moments M_0

Let $2\vartheta_0$ denote the span of an arc of radius $R = 1$ subject to constant bending moments M_0 (see Fig. 1).

	$GD/(M_0^2R)$	rel. err.		$GD/(M_0^2R)$	rel. err.
Exact 20°	.4711E+00		Exact 70°	.1476E+01	
M_{10}, 20°	.5014E+00	.643E-01	M_{10}, 70°	.1416E+01	-.409E-01
M_{20}, 20°	.4522E+00	-.401E-01	M_{20}, 70°	.1417E+01	-.400E-01
S_{10}, 20°	.4712E+00	.227E-03	S_{10}, 70°	.1477E+01	.224E-03
S_{20}, 20°	.4714E+00	.566E-03	S_{20}, 70°	.1477E+01	.564E-03

Table 4: Arc crack: adimensional energy release rates

The stress intensity factors are (Sih, 1973):

$$k_1 = -\frac{6M_0(1-\nu)}{h^2}e^{\pi\vartheta_0}C_0\sqrt{\sin\vartheta_0}\cos\frac{\vartheta_0}{2} \qquad k_2 = -\frac{6M_0(1-\nu)}{h^2}e^{\pi\vartheta_0}C_0\sqrt{\sin\vartheta_0}\sin\frac{\vartheta_0}{2}$$

where:

$$C_0 = -\frac{2(3+\nu)}{\cos\vartheta_0(1-\nu)+5+3\nu}$$

Two different values for ϑ_0 are considered: 20° and 70°. In each case four meshes are tested: M_{10}, ϑ_0 and M_{20}, ϑ_0 with ten and twenty linear elements respectively; S_{10}, ϑ_0 and S_{20}, ϑ_0 always with ten and twenty linear elements but with special elements. The results are presented in Table 3 and Table 4.

REFERENCES

Aliabadi, M.H. and D.P. Rooke (1991). *Numerical Fracture Mechanics.* Kluwer Academic Press, Dordrecht.

Bonnet, M. (1996). Regularized BIE formulations for first- and second- order shape sensitivity of elastic fields, *Computer & Structures.* submitted.

Dems, K. and Z. Mróz (1984). Variational approach by means of adjoint systems to structural optimization and sensitivity analysis: structure shape variation, *Int. J. Solids Structures.* 20, 527-552.

Frangi, A. (1996). A new regularized BE formulation for Kirchhoff plates, *Eur. J. Mech., A/Solids.* in press.

Frangi, A. and M. Bonnet (1996). A Galerkin symmetric and direct BIE method for Kirchhoff elastic plates: formulation and implementation, *Int. J. Num. Meth. Engng..* submitted.

Frangi, A. and G. Novati (1996). Symmetric BE method in two dimensional elasticity: evaluation of double integrals for curved elements, *Computat. Mech..* submitted.

Frangi, A. (1997). Computation of energy release rates for cracks in thin plates through a symmetric BE approach, *Journal of Fracture.* in preparation.

Hui, C.Y. and A.T. Zehnder (1993). A theory for the fracture of thin plates subjected to bending and twisting moments, *Journal of Fracture.* 61, 211-229.

Maier, G. and C. Polizzotto (1987). A Galerkin approach to boundary elements elastoplastic analysis, *Comp. Meth. Appl. Mech. Engng..* 60, 175-194..

Maier, G., Z. Cen and G. Novati (1993). Symmetric Galerkin boundary element method for quasi-brittle fracture and frictional contact problems, *Computat. Mech..* 13, 74-89.

Nishimura, N. and S. Kobayashi (1991). A boundary integral equation method for an inverse problem related to crack detection, *Int. J. Num. Meth. Engng..* 32, 1371-87.

Portela, A. (1993). *Dual Boundary Element Analysis of Crack Growth.* Computational Mechanics Publications, Southampton.

Sirtori, S. (1979). General stress analysis method by means of integral equations and boundary elements, *Meccanica.* 14, 210-218.

Sirtori, S., G. Maier, G. Novati and S. Miccoli (1992). A Galerkin symmetric boundary element method in elasticity: formulation and implementation, *Int. J. Num. Meth. Engng..* 35, 255-282.

Sih, G.C. (1973). *Handbook of Stress Intensity Factors.* Lehigh University, Bethlehem.